

Parametric Transition as a Spiral Curve and Its Application in Spur Gear Tooth with FEA

S. H. Yahaya, J. M. Ali and T.A. Abdullah

Abstract—The exploration of this paper will focus on the C-shaped transition curve. This curve is designed by using the concept of circle to circle where one circle lies inside other. The degree of smoothness employed is curvature continuity. The function used in designing the C-curve is Bézier-like cubic function. This function has a low degree, flexible for the interactive design of curves and surfaces and has a shape parameter. The shape parameter is used to control the C-shape curve. Once the C-shaped curve design is completed, this curve will be applied to design spur gear tooth. After the tooth design procedure is finished, the design will be analyzed by using Finite Element Analysis (FEA). This analysis is used to find out the applicability of the tooth design and the gear material that chosen. In this research, Cast Iron 4.5 % Carbon, ASTM A-48 is selected as a gear material.

Keywords—Bézier-like cubic function, Curvature continuity, C-shaped transition curve, Spur gear tooth.

I. INTRODUCTION

CURVE design is one of the vital parts in Computer Aided Geometric Design (CAGD). Curve design is used to create the right curve with all the properties of designing the curve are satisfied. The process will be continued to apply this generated curve in practical base such in industrial application. In this paper, we would like to design a C-shaped transition curve by using a Bézier-like cubic function and will apply to spur gear tooth design. This C-shaped curve will be designed by using the design templates proposed by Baass [1].

One of the templates in Baass [1] is circle to circle where one circle lies inside the other circle with a C transition curve. The concept of this template will be applied in this paper. The Bézier-like cubic function is used because it has a low degree polynomial curve and suitable in Computer Aided Design (CAD) application. This function is written in Bézier form for its geometric property, numerical property and easy to use and implement. For many years, an involute curve application has been used in designing and generating a spur gear tooth. The tracing point method is used to design this involute curve while a C-shaped curve can directly produce the curve. Many

researchers have been connected in this area like Walton and Meek [2]–[6] have discussed about planar G^2 transition between two circles with fair cubic Bézier curve, the use of cornu spirals in drawing planar curves of controlled curvature, planar G^2 transition curves composed of cubic Bézier spiral segments, curvature extrema of planar parametric polynomial cubic curves and a planar cubic Bézier spiral. This also includes about G^2 cubic transition between two circles with shape control, circle to circle transition with a single cubic spiral and G^2 planar cubic transition between two circles are written by Habib and Sakai [7]–[9].

This paper consists of the background, notation and convections, followed by the explanation of Bézier-like cubic function. This paper will carry on the design of a C-shaped transition curve by applying one circle lies inside other circle template with numerical example will be shown. Spur gear tooth design using a C-shaped transition curve application will be demonstrated in the next part, continued by spur gear analysis. Finally, conclusions and several recommendations for future work.

II. BACKGROUND, NOTATION AND CONVECTIONS

Consider the Cartesian coordinate system such as vector, $\mathbf{A} = (A_x, A_y)$. The Euclidean norm or length of vector, \mathbf{A}

is formulated by $\|\mathbf{A}\| = \sqrt{(A_x^2 + A_y^2)}$.

An angle measured in this paper is anti-clockwise angle. The derivative of a function, f is denoted by f' . The dot product of two vectors, \mathbf{A} and \mathbf{B} is written as $\mathbf{A} \cdot \mathbf{B}$. A planar parametric curve is defined by a set of points, $z(t) = (x(t), y(t))$ with t given in real line interval. In this paper, we use $t \in [0,1]$.

The cross product of two vectors, \mathbf{A} and \mathbf{B} is defined by $\mathbf{A} \wedge \mathbf{B} = A_x B_y - A_y B_x = \|\mathbf{A}\| \|\mathbf{B}\| \sin \theta$ where, θ is anti-clockwise angle and the symbol, “ \wedge ” is used as cross product expression, as described in Juhász [10]. The tangent vector of a plane parametric curve is stated by $z'(t)$. If $z'(t) \neq 0$ then the definition of curvature, $z(t)$ can be defined as,

S. H. Yahaya is with the Manufacturing Engineering Faculty, University of Technical Malaysia Melaka, 76109, Melaka, Malaysia (phone: 606-331-6494; fax: 606-331-6431; e-mail: saifudin@utem.edu.my).

J. M. Ali is with the School of Mathematical Sciences, University of Science Malaysia, 11800, Penang, Malaysia. (e-mail: jamaluma@usm.my).

T. A. Abdullah is with the Manufacturing Engineering Faculty, University of Technical Malaysia Melaka, 76109, Melaka, Malaysia (e-mail: tajul@utem.edu.my).

$$\kappa(t) = \frac{z'(t) \wedge z''(t)}{\|z'(t)\|^3} \quad (1)$$

Equation (1) will be differentiated as,

$$\kappa'(t) = \frac{\omega(t)}{\|z'(t)\|^5} \quad (2)$$

where,

$$\omega(t) = \|z'(t)\|^2 \frac{d}{dt} \{z'(t) \wedge z''(t)\} - 3\{z'(t) \wedge z''(t)\} \{z'(t) \cdot z''(t)\} \quad (3)$$

The term “transition curve” can be defined as a special curve where the degree of curvature is varied to give a gradual transition between a tangent and a simple curve or between two simple curves which the connection happened.

III. BEZIER-LIKE CUBIC FUNCTION

A planar Bézier-like cubic function is developed by Ali et al. [11] as presented below:

$$z(t) = ((1-t)^2(1+t(2-\lambda_0)))P_0 + (\lambda_0(1-t)^2t)P_1 + (\lambda_1(1-t)t^2)P_2 + (t^2(1+(1-t)(2-\lambda_1)))P_3, t \in [0,1] \quad (4)$$

where P_0, P_1, P_2, P_3 are the control points and λ_0, λ_1 are the parameters controlling the curve shape. In this paper, the value of $\lambda_0, \lambda_1 \in (0,3)$ to guarantee the Bézier-like cubic function has a constant sign of curvature either positive or negative.

IV. CIRCLE TO CIRCLE WITH A SINGLE SPIRAL

A C-shaped transition curve is applied to join these two circles. Referring to Habib and Sakai [9], the control points used in this circle to circle template are:

$$\begin{aligned} P_0 &= c_0 + (r_0 * t_0), P_1 = P_0 + (h * t_1), \\ P_2 &= P_3 + (k * t_2), P_3 = c_1 - (r_1 * t_3) \end{aligned} \quad (5)$$

with the knot points are,

$$\begin{aligned} t_0 &= \{\cos[\alpha], \sin[\alpha]\}, t_1 = \{-\sin[\alpha], \cos[\alpha]\}, \\ t_2 &= \{\sin[\beta], \cos[\beta]\}, t_3 = \{\cos[\beta], -\sin[\beta]\} \end{aligned} \quad (6)$$

where, c_0, r_0 and α are the center point, radius and angle of big circle, Ω_0 . For small circle, Ω_1 , the parameters involved are c_1, r_1 and β representing center point, radius and angle of

this small circle while $h = \|P_1, P_0\|$ and $k = \|P_3, P_2\|$.

This concept will be involving two segments of curves to design a C-shaped curve. For this reason, it is not guarantee that this C-shaped curve is a single spiral. The modification of this concept is needed to ensure that C-shaped curve is a single spiral curve. The idea of modification will be looking at the curve segment where this segment will be reduced to be one curve segment.

Let we modify the control and knot points in (5) and (6) to be rewritten as,

$$\begin{aligned} P_0 &= c_0 - (r_0 * t_0), P_1 = P_0 + (k * t_1), \\ P_2 &= P_3 - (h * t_2), P_3 = c_1 + (r_1 * t_3) \end{aligned} \quad (7)$$

and,

$$\begin{aligned} t_0 &= \{\cos[\beta], \sin[\beta]\}, t_1 = \{\sin[\beta], -\cos[\beta]\}, \\ t_2 &= \{-\sin[\alpha], \cos[\alpha]\}, t_3 = \{\cos[\alpha], \sin[\alpha]\} \end{aligned} \quad (8)$$

Then, we make an assumption where $P_1 = P_2$ in (7) and (8). By applying the dot product of vector, we eliminate h to get,

$$k = \frac{((c_1 - c_0) \cdot \{\cos[\alpha], \sin[\alpha]\}) + r_1 + (r_0 * \cos[\alpha - \beta])}{\sin[\beta - \alpha]} \quad (9)$$

and the new control points are:

$$\begin{aligned} P_0 &= c_0 - (r_0 * \{\cos[\beta], \sin[\beta]\}), \\ P_1 &= P_0 + (k * \{\sin[\beta], -\cos[\beta]\}), \\ P_2 &= c_1 + (r_1 * \{\cos[\alpha], \sin[\alpha]\}). \end{aligned} \quad (10)$$

The joining curve between these two circles is generated by using curvature continuity where this continuity condition must be satisfied. The conditions are;

$$\kappa(t=0) = \frac{1}{r_0}, \kappa(t=1) = \frac{1}{r_1} \quad (11)$$

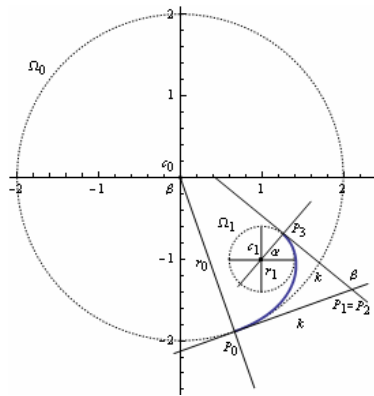


Fig. 1 Circle to circle where one circle lies inside the other circle with a C-shaped transition curve

Next, numerical example will be demonstrated to ensure the theoretical above.

V. NUMERICAL EXAMPLE

Let we have center points, $c_0 = \{0,0\}$, $c_1 = \{1,-1\}$, radius, $r_0 = 2$, $r_1 = 0.4$ and angles, $\alpha = 0.8217$ radian, $\beta = 1.9201$ radian.

By applying (10), we determine $k = 1.4135$, and the shape parameters are calculated by using (1), (10) and (11) where the values are; $\lambda_0 = 1.8733$ and $\lambda_1 = 1.0546$. This example will be visualized in Fig. 2.

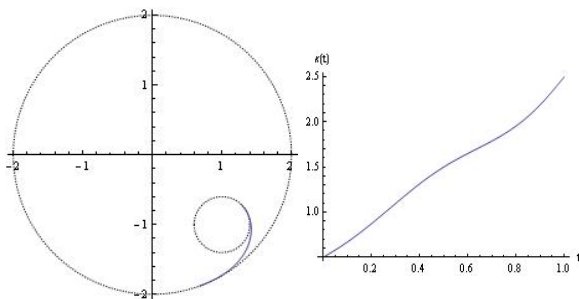


Fig. 2 Example of circle to circle problem with its curvature profile

Fig. 2 has a positive curvature where we can see clearly from its curvature profile. Hence, the generated curve can be described as a spiral curve. Next, the application of this circle problem is used to design the shape of spur gear tooth.

VI. SPUR GEAR TOOTH DESIGN

An involute curve usually used to design a spur gear tooth. The tracing point method is employed to generate this curve. In this paper, circle to circle with a C transition curve scheme will be applied in spur gear tooth design. This scheme can directly produce curve.

Let consider the center point of two circles is denoted as $c = \{0,0\}$ and its radius, $r_0 = 1$ and $r_1 = 0.588$. Inside these

two circles, we make the circle division where each circles have radius, $r = 0.206$. For the connecting these circles, we design another circle division with radius, $r_c = 0.05$. This circle model can be seen clearly in Fig. 3.

The next procedure will focus on the connection between these circles. In order to do that, we divide the circle model into four segments.

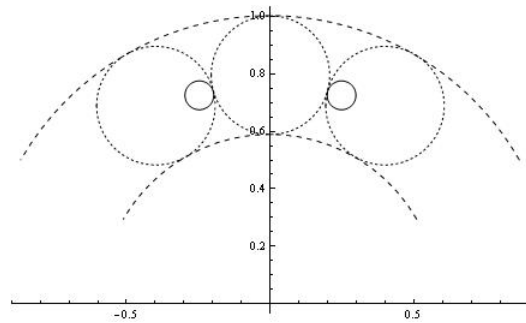


Fig. 3 Circle model is used to design spur gear tooth

In first segment, the inputs are; $\alpha = 0.1745$ rad, $\beta = 2.0944$ rad, $c_0 = \{-0.3980, 0.6890\}$, $c_1 = \{-0.2470, 0.7250\}$, $r_0 = 0.2060$, $r_1 = 0.0500$. By applying (9), k equivalents to 0.1431 while $\{\lambda_0, \lambda_1\} = \{2.7695, 0.3619\}$ is obtained by using (1), (10) and (11).

For second segment, we have $\alpha = 4.7124$ rad, $\beta = 0.1745$ rad, $c_0 = \{0.0000, 0.7950\}$, $c_1 = \{-0.2470, 0.7250\}$, $r_0 = 0.2060$, $r_1 = 0.0500$. Then, $\{k, \lambda_0, \lambda_1\} = \{0.2449, 2.1279, 0.5343\}$ is determined by using the same approach as in first segment.

The third and four segments are symmetry to segment 1 and 2 where the mirroring technique has been applied to create the joining curve. The result is shown in Fig. 4.

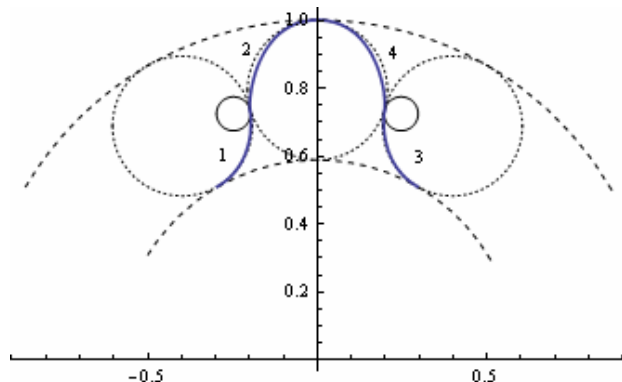


Fig. 4 Spur gear tooth design using a C-shape curve application

This work will extend to develop the spur gear model. This spur model can be used easily in 3D modeling analysis approach. We have two options in creating a model either using Mathematica 6.0 or Catia V5 software. In this paper, we have chosen Catia V5 because of this engineering software is easy to handle and practical to use in solid modeling.

For remaining the gear tooth shape in Fig. 4, method of coordinate selection will be applied. Mathematica 6.0 has several drawing tools in graphics palette. One of the tools is “get coordinates” tool as shown in Fig. 5. We click the “get coordinates” tool and the mouse pointer over the 2D graphics or plot.

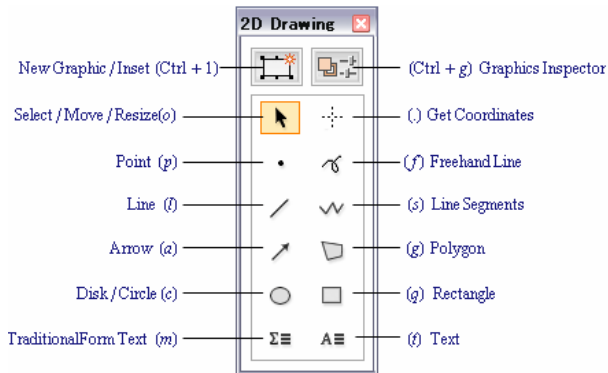


Fig. 5 2D drawing tool in Mathematica 6.0

The approximate coordinate values of mouse pointer are displayed. Then, click at the marker to mark the coordinate. In order to add marker, we can click to other position. As an example, see in Fig. 6.

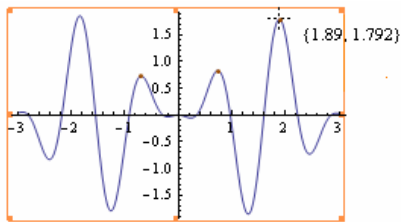


Fig. 6 Coordinates selection using “get coordinates” tool

Finally, use Ctrl+C to copy the marked coordinates and Ctrl+V to paste these coordinates into an input cell as demonstrated in Fig. 7.

{{1.89, 1.792}, {0.7403, 0.8351}, {-0.6706, 0.7132}}

Fig. 7 List of coordinates in an input cell

In this work, 38 coordinates have been selected to design a spur gear model. We also set the gear thickness equivalents to 4.0000 mm and the radius of gear shaft is 2.8360 mm. In designing this gear model, we join all the coordinates by using the spline package which the package comprised in Catia V5 software. The visualization of this model is shown in Fig. 8.

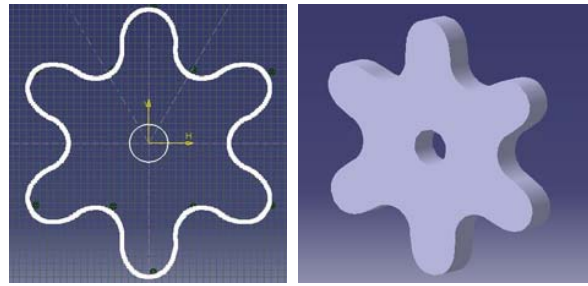


Fig. 8 Spur gear model displayed in 2D (left) and 3D (right)

After getting the gear model, static and strength analysis will be touched upon in this paper. In engineering field, this analysis process is under Computer Aided Engineering (CAE). The detail explanations about this analysis will be explained in the next section.

VII. SPUR GEAR ANALYSIS

The main intention of this section is to find out an applicability of gear tooth design with the material used. For the beginning, static and strength analysis is used because of this strength analysis appropriates to the design structure. Nastran/Patran is software used in this analysis. The following flow chart is applied in this spur analysis.

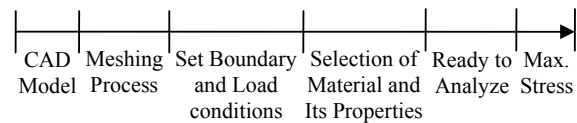


Fig. 9 Algorithms in spur gear analysis

The analysis process is began by importing the gear model (Fig. 8) into Nastran/Patran software such as,

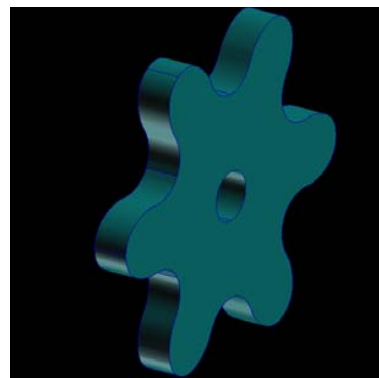


Fig. 10 Smooth shaded gear model in Nastran/Patran software

The gear structure in Fig. 10 is a 3D geometry solid model exposing a complex structure. Solid element models are typically used to analyze a complex structural component, to apply a complex loading condition and forecast the stress level. In this structure, the suitable element topology applied is

Tetrahedral-10 (Tet-10) represents a 3D solid triangle with 4 planar faces and 10 nodes. The reason of choosing this topology is its ability to mesh almost any solid regardless of its complexity. The meshing process is done by using Patran software where FEA application is used. The Finite Element Model (FEM) for this spur model consists of 36356 nodes and 23683 elements where global edge length employed is 1.0.

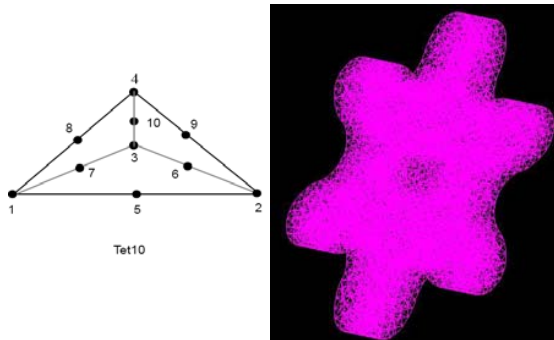


Fig. 11 Tet-10 (left) and its application to spur gear model (right)

The next procedure will focus on the setting of boundary and loading conditions in the model. Boundary conditions are placed in the gear shaft because in this shaft area, the nodal displacement would not be happened. The loading condition is located in gear contact area. Note that this area will be connected to other gear. The location will be around the gear tooth set. The reason of choosing this location is to find out whether the tooth design can remain the same from any heavy impact. This is very important setup in order to complete this static analysis. As an example, we apply the load equivalents to 5000 N. The details, see in Fig. 12.

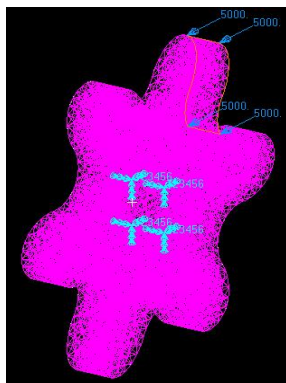


Fig. 12 Loading and boundary conditions in spur gear model

The next procedure is to select the suitable material in this gear model. In gear manufacturing, there is several gear materials available such as Cast Steel, Cast Iron, Alloy Steel and Stainless Steel. In this paper, the material chosen is Cast Iron 4.5 % Carbon, ASTM A-48. This gear material is highly recommended in gear manufacturing because it is low of manufacturing cost, easy to machine and good machining characteristics. The detail characteristics of this gear material

are shown in Table I.

Table I shows the Cast Iron properties. These properties will be used as the inputs to run Nastran/Patran software.

TABLE I
CAST IRON 4.5 % CARBON, ASTM A-48 CHARACTERISTICS

Young's Modulus (GPa)	Yield Strength (MPa)	Poisson Ratio
211	130	0.27

Thus, spur gear model is ready to analyze. The model is run by using the computer with 256 MB RAM and processor Intel (R), Pentium (R) 2.4 GHz. The computer required ± 13 minutes to run the full-gear model with the load applied is 5000 N.

We discover that the maximum von mises stress is 696 Pa occurred in the gear shaft at node 27625 while the minimum stress is 0.0641 Pa at node 29648. This minimum stress happened along the tooth set in the model. The result can be seen clearly in Fig. 13.

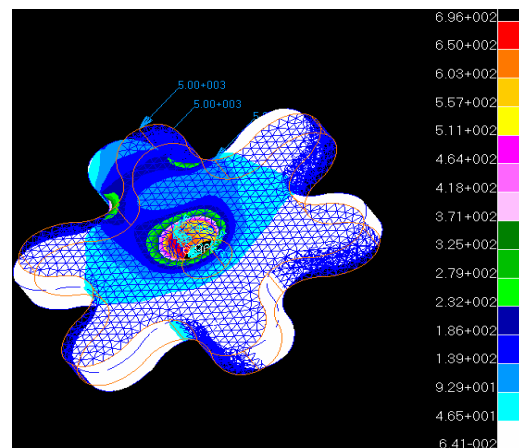


Fig. 13 Von Mises stress distribution in spur gear model

The yield strength of Cast Iron 4.5 % Carbon, ASTM A-48 material is 130 MPa while the maximum stress calculated by the simulation is 696 Pa. It is obviously shows the maximum stress obtained from the simulation is far below compared to the material's yield strength. The following calculation is used to calculate the safety factor of this spur model. This safety factor is denoted as,

$$\sigma = \frac{\text{Yield strength of material}}{\text{Maximum Von Mises stress}} \quad (12)$$

For the load equivalents to 5000 N, the σ approximates to 1.90E05 where the units for both sides in (12) must be same. Consider the material and design failure occurred if $\sigma \leq 1$, it is noted that the failure will not occur in this load. Therefore, the design of spur gear and the material applied are safe to use for the load equals to 5000 N. In this paper, we have tested the various loads which the objective is to find out when the

design and the material applied fail to be used. The findings are shown in Table II.

In Table II, we can see clearly that the design and material applied are in failure condition when the load $\geq 1.0\text{E}09$ N. Otherwise, the design and material applied are in safety

TABLE II
SAFETY FACTOR WITH DIFFERENT LOADS

Total Loads (N)	Maximum Von Mises Stress (Pa)	Safety Factor, σ
5.00E06	6.96E05	186.78
7.00E07	9.75E06	13.33
8.00E08	1.11E08	1.17
9.00E08	1.25E08	1.04
1.00E09	1.39E08	0.94

condition. In this paper, we also do the comparison study with an existing design. The material used in this existing design is same as new design above. This existing design is designed directly using engineering graphic concept.

As a result, the failure happened in the existing design when load $\geq 1.0\text{E}09$ N. It shows that the new and existing designs are both have the same structure strength. In other aspect, the new design will give another alternative to the designers or manufacturers use and the important is that the C-shaped curve application can be applied in gear tooth shape especially, in spur gear.

The next procedure, we would like to extend these results in order to identify the fatigue condition for both designs.

VIII. FATIGUE ANALYSIS

In engineering field, fatigue can be described as a failure condition happened on the structure design affected from the implications of repeated or varying loads. The intention of this section is to find out when the fatigue starts to occur in the both designs above.

As mentioned earlier, the design fails to be used when the $\sigma \leq 1$. From this inequality, we understand that $\sigma < 1$ and $\sigma = 1$. Thus, we assume that the fatigue starts to happen when σ equals to 1. Next, will be the calculation on the related load due to this σ .

In order to do that, the interpolation technique is applied. This technique is based on the Taylor series expansion and very useful in data prediction. Consider the following n th-order polynomial interpolation can be expressed as,

$$f_n(x) = a_0 + a_1(x - x_0) + a_2(x - x_0)(x - x_1) + a_3(x - x_0)(x - x_1)(x - x_2) + \dots + a_n(x - x_1) \dots (x_n - x_{n-1}) \quad (13)$$

where, n is the order of polynomial, a_0, a_1, \dots, a_n are the polynomial coefficients and the $(n + 1)$ data points, $\{x_i, f(x_i)\}$ with $i = 0, 1, 2, 3, \dots, n$. These coefficients can be evaluated using all these points.

Equation (13) also known as the n th-order Newton's divided-difference interpolating polynomial. Let develop the first-order Newton interpolation ($n = 1$). Thus, we need two data points and obtain,

$$a_0 = f(x_0), a_1 = \frac{f(x_1) - f(x_0)}{x_1 - x_0} \quad (14)$$

Then, the first-order Newton's polynomial can be written as,

$$f_1(x) = a_0 + a_1(x - x_0) \quad (15)$$

By referring to Table II, we set the total loads as in x -axis and safety factor as in y -axis or $f(x)$ because x -axis is known as an input factor while y -axis as an output factor. As explained before, the design and material applied fail to be used between the range of $9.00\text{E}08$ N to $1.00\text{E}09$ N. Thus, a_0 and a_1 can be computed by using (14) where,

$$a_0 = 1.04, a_1 = -1.00\text{E} - 09 \quad (16)$$

These values in (16) can be used in developing the first-order Newton's polynomial as,

$$f_1(x) = 1.04 - 1.00\text{E} - 09 * (x - 9.00\text{E}08) \quad (17)$$

By setting $f_1(x) = 1$, we solve (17) to estimate,

$$x \approx 9.40\text{E}08 \text{ N} \quad (18)$$

According to this analysis, the design and material applied are considering in safety mode if the load $< 9.40\text{E}08$ N while the design starts to fail to be used if the load $\geq 9.40\text{E}08$ N. For an existing design, we obtain the same optimization after compared with the new design. It shows that the new and existing design have similar fatigue life to keep these designs from various impacts.

IX. CONCLUSION AND RECOMMENDATIONS

In this paper, we have shown that case fifth explained by Baass [1] can be used and applied in designing and also producing a spur gear tooth design, absolutely in generating the tooth shape. We are completely demonstrate the structural analysis used in this spur design. In predicting the fatigue life for the design and material, we have used the interpolation technique where this technique is easy to apply and handle. The important is that case fifth can be applied as an optional method for designers or manufacturers in designing gears. In future, we are interesting to continue this research in dynamic feature and the acoustic phenomenon test. Once all the analyses have been done, we also interested to do the fabrication process in this spur gear design.

ACKNOWLEDGMENT

This research is supported by the Department of Higher Education, Malaysia and UTeM under FRGS grant. The authors gratefully acknowledge to everybody for their helpful comments.

REFERENCES

- [1] K. G. Baass, "The use of clothoid templates in highway design," *Transportation Forum 1*, 1984, pp. 47–52.
- [2] D. J. Walton, and D. S. Meek, "Planar G^2 transition between two circles with a fair cubic Bézier curve," *J. Computer Aided Design*, 31, 1999, pp. 857–866.
- [3] D. J. Walton, and D. S. Meek, "The use of cornu spirals in drawing planar curves of controlled curvature," *J. Computational and Applied Mathematics*, 25, 1989, pp. 69–78.
- [4] D. J. Walton, D. S. Meek, and J. M. Ali, "Planar G^2 transition curves composed of cubic Bézier spiral segments," *J. Computational and Applied Mathematics*, 157, 2003, pp. 453–476.
- [5] D. J. Walton, and D. S. Meek, "Curvature extrema of planar parametric cubic curves," *J. Computational and Applied Mathematics*, 134, 2001, pp. 69–83.
- [6] D. J. Walton, and D. S. Meek, "A planar cubic Bézier spiral," *J. Computational and Applied Mathematics*, 72, 1996, pp. 85–100.
- [7] Z. Habib, and M. Sakai, " G^2 planar cubic transition between two circles with shape control," *J. Computational and Applied Mathematics*, 223, 2009, pp. 133–144.
- [8] Z. Habib, and M. Sakai, "Circle to circle transition with a single cubic spiral," *Proc. Int. Conf. on Visualization, Imaging, and Image Processing*, ACTA Press, 2005, pp. 691–696.
- [9] Z. Habib, and M. Sakai, " G^2 planar cubic transition between two circles," *Int. J. Computer Mathematics*, 80, 2003, pp. 959–967.
- [10] I. Juhász, "Cubic parametric curves of given tangent and curvature," *J. Computer Aided Design*, 25, 1998, pp. 1–9.
- [11] J. M. Ali, H. B. Said, and A. A. Majid, "Shape control of parametric cubic curves," *Proc. Fourth Int. Conf. CAD/CG*, 1995, pp. 161–166.
- [12] B. W. Bair, "Computer aided design of elliptical gears," *J. Mechanical Design*, 124, 2002, pp. 787–793.
- [13] G. I. Sheveleva, A. E. Volkov, and V. I. Medvedev, "Algorithm for analysis of meshing and contact of spiral bevel gears," *J. Mechanism and Machine Theory*, 42, 2006, pp. 198–215.
- [14] A. Belsak, and J. Flaker, "Method for detecting fatigue crack in gears," *J. Theoretical and Applied Fracture Mechanics*, 46, 2006, pp. 105–113.